

Original citation:

Yuan, Hu, Guo, Weisi, Jin, Yanliang, Wang, Siyi and Ni, Minming. (2017) Interference-aware multi-hop path selection for device-to-device communications in a cellular interference environment. IET Communications.

Permanent WRAP URL:

<http://wrap.warwick.ac.uk/87352>

Copyright and reuse:

The Warwick Research Archive Portal (WRAP) makes this work by researchers of the University of Warwick available open access under the following conditions. Copyright © and all moral rights to the version of the paper presented here belong to the individual author(s) and/or other copyright owners. To the extent reasonable and practicable the material made available in WRAP has been checked for eligibility before being made available.

Copies of full items can be used for personal research or study, educational, or not-for-profit purposes without prior permission or charge. Provided that the authors, title and full bibliographic details are credited, a hyperlink and/or URL is given for the original metadata page and the content is not changed in any way.

Publisher's statement:

"This paper is a postprint of a paper submitted to and accepted for publication in IET Communications and is subject to Institution of Engineering and Technology Copyright. The copy of record is available at IET Digital Library"

A note on versions:

The version presented here may differ from the published version or, version of record, if you wish to cite this item you are advised to consult the publisher's version. Please see the 'permanent WRAP URL' above for details on accessing the published version and note that access may require a subscription.

For more information, please contact the WRAP Team at: wrap@warwick.ac.uk

Interference-Aware Multi-Hop Path Selection for Device-to-Device Communications in a Cellular Interference Environment

Hu Yuan¹, Weisi Guo^{1*}, Yanliang Jin², Siyi Wang³, Minming Ni⁴

¹School of Engineering, University of Warwick, UK

²School of Communication and Information Engineering, Shanghai University, China.

³Department of Electrical and Electronic Engineering, Xi'an Jiaotong-Liverpool University, China.

⁴School of Electronic and Information Engineering, Beijing Jiaotong University, China.

*weisi.guo@warwick.ac.uk

Abstract: Device-to-Device (D2D) communications is widely seen as an efficient network capacity scaling technology. The co-existence of D2D with conventional cellular (CC) transmissions causes unwanted interference. Existing techniques have focused on improving the throughput of D2D communications by optimising the radio resource management and power allocation. However, very little is understood about the impact of the route selection of the users and how optimal routing can reduce interference and improve the overall network capacity. In fact, traditional wisdom indicates that minimising the number of hops or the total path distance is preferable. Yet, when interference is considered, we show that this is not the case. In this paper, we show that by understanding the location of the user, an interference-aware routing algorithm can be devised. We propose an adaptive Interference-Aware-Routing (IAR) algorithm, that on average achieves a 30% increase in hop distance, but can improve the overall network capacity by 50% whilst only incurring a minor 2% degradation to the CC capacity. The analysis framework and the results open up new avenues of research in location-dependent optimization in wireless systems, which is particularly important for increasingly dense and semantic-aware deployments.

1. Introduction

In recent years, the cellular network has experienced significant growth in wireless data demand (an average 66% Compound Annual Growth Rate) and is at risk of not being able to meet the demand in the near future. Indeed there is a widespread recognition that the average network capacity needs to grow by 1000-fold over the coming decade and the minimum achievable capacity needs to grow by 10-fold.

1.1. Background to D2D

Device-to-Device (D2D) communications, which is part of the LTE-Direct standard, is a technique of allowing user equipment (UEs) to communicate directly with each other, using neighbouring UEs as relays [1]. When we consider this in the context of an existing cellular infrastructure, an overlay of macro base stations (BSs) will provide overall signal coverage and control for D2D operations (i.e., cellular assisted D2D access). Therefore, at any particular instance, the UEs that participate in D2D communications can be perceived as forming the underlay of a temporary het-

erogeneous network [2, 3]. The conditions which might trigger establishing cellular assisted D2D communications include insufficient channel resources in the BS and the transmission of delay tolerant data [2]. As for device discovery between potential D2D UEs, it has been proposed that the UEs can utilize recent 3GPP proximity services (ProSe) standardisation [4]. D2D communications also enable distributed storage [5] and relate the natural way in which people interact and exchange information socially [6, 7]. Due to the multi-hop nature of D2D relaying, the Quality-of-Service (QoS) performance metrics associated with D2D communications are primarily related to outage probability, as the data is usually for services that demand a low data rate and can tolerate a high latency.

1.2. Review of Multi-Hop Optimization

Stand-alone multi-hop routing in wireless communications is a well addressed research area. In the past, research has focused on: i) how to incorporate feedback mechanisms to ensure greater routing reliability [8], ii) how to optimise partner selection to exploit spatial diversity [9–11] and iii) how to optimise spectrum sharing and power control for increased energy- and spectrum efficiency [2, 3, 12]. However, when one considers multi-hop routing in the context of D2D communications, a major modelling consideration is the mutual interference between the overlay macro-BS tier and the temporarily formed underlay D2D tier. One of the unresolved, and must be resolved challenges is, how to efficiently select D2D relay partners in such an interference-limited environment. This is a dynamic problem with many variables such as the location of the source-destination UE pair.

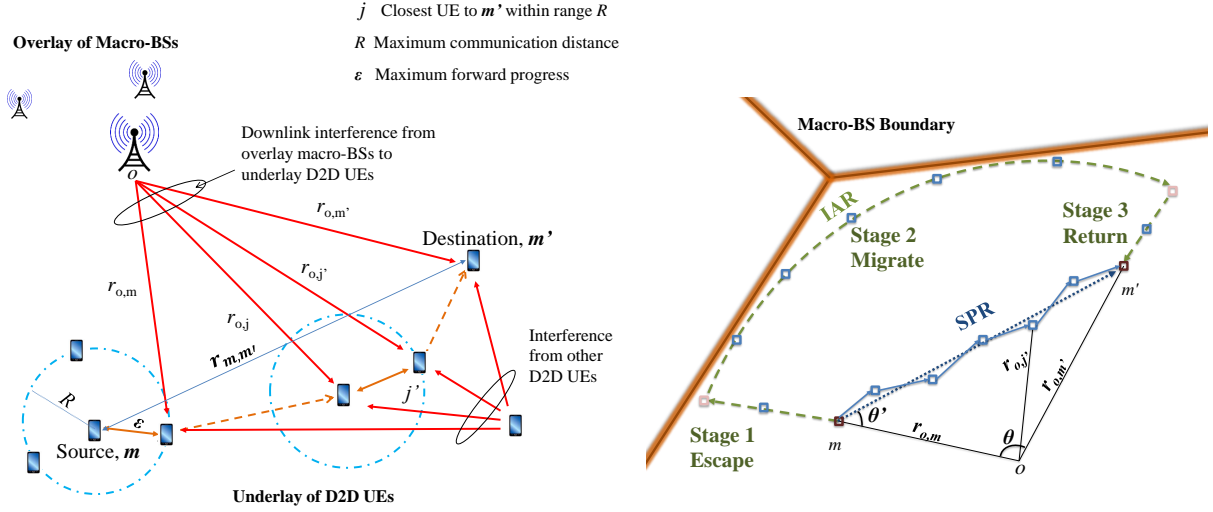
In terms of existing work on multi-hop routes that mitigate cross-tier interference, one approach used is to introduce and optimise an artificial exclusion zone, where D2D transmissions can occur only inside the zone, and CC transmissions are restricted to outside the zone [13]. The caveat with this approach is that a large number of exclusion zones can severely degrade CC transmission capacity. The other approach is one in which we proposed ourselves. This approach is one where the routing path is dynamically controlled such that it spatially avoids high cross-tier interference areas. This is known as Interference-Aware-Routing (IAR), and we conducted a preliminary numerical analysis in [14]. We note that similar ideas have also been presented subsequently in [15] and has shown promising results.

1.3. Stochastic Geometry Modelling

We also briefly review general modelling methodologies. This paper employs both large-scale statistical modelling in the form of stochastic geometry, as well as agent-based-modelling (ABM) using Monte-Carlo cellular network simulations. In reviewing stochastic geometry analysis, it can obtain general performance analysis, guidelines, and design insights that apply when averaging over all distinct realisations [16, 17]. This complements our ABM models, which utilises standard 4G LTE spatial and protocol configurations for the macro-BS cellular network and D2D underlay network [14].

1.4. Contribution and Organisation

This paper proves that a longer multi-hop route that can reduce cross-tier interference between BS and D2D transmissions can significantly improve overall system performance. We compare the proposed Interference-Aware-Routing (IAR) algorithm with classical greedy Shortest Path Routing (SPR) algorithms. Methodologically, this paper attempts, for the first time, (1) to provide a stochastic geometry theoretical framework mathematical to generalise the performance compari-



(a) An overlay of macro-BSs and an underlay of D2D UEs performing multi-hop communications from UE m to UE m' . The maximum potential forwarding distance within D2D UEs coverage boundary for each single hop.

(b) D2D multi-hop communications from m to m' under SPR or IAR algorithms.

Fig. 1. Routing algorithms for D2D multi-hop communications.

son, (2) provide geometric boundaries that define the spatial operational envelopes for different D2D routing algorithms and CC transmissions, and (3) analyse the downlink (DL) system performance (outage probability and capacity) as a function of the offloaded traffic volume.

The paper is organised as follows. In Section II, the system setup and parameters used for ABM simulation and stochastic geometry framework are defined. The two main routing algorithms (SPR and IAR) are defined in section III. In Section IV, the performance metrics for both algorithms are defined and their theoretical bounds are derived. In Section V, the results on network capacity, offload traffic volume, and outage probability are presented together as well as the relationship to spatial operating zones. [In Section VI, we conclude our findings and discuss open challenges.](#)

2. System Setup

[The system modelled in this paper is a 4G multiple-access network with cellular BS assisted access D2D communications.](#) The D2D communication links can utilise either the in-band cellular spectrum or out-band spectrum ([pre-defined, i.e., LTE-U \[18\]](#)). Due to the scarcity of the spectrum and the transmission regulations in unlicensed bands, the in-band case is selected for analysis, where low power D2D communications share the same spectrum as the conventional cellular (CC) channels [1, 2]. In general, the centre of the BS's coverage area is off-limits to D2D transmissions using the cellular DL band due to the high DL interference from the nearby macro-BS. The cell edge is generally off-limits to D2D transmissions using the cellular UL band due to the high UL interference from cell-edge CC UEs transmitting at high power levels. As shown in Fig. 1(a), D2D UEs share the DL spectrum with the CC network, and as a result, DL interference is from the overlay macro-BSs to underlaying D2D UEs.

The general D2D communications involves a source UE m' employing multi-hop communication to relay data to destination UE m' via relay UEs j . In this paper, the analysis only considers

the multi-hop communication between two arbitrarily located UEs within the coverage area of a BS, but Section V will discuss how it can be extended to consider the communication between two UEs that are not in the same coverage area of a single BS. We consider both the BSs and UEs are distributed randomly uniformly, i.e., a Poisson Point Process (PPP) with the density Λ_{D2D} , and BSs are distributed as a PPP with density of Λ_{BS} [19]. The traffic in the network is assumed to be full buffer (i.e., every radio-resource-block (RRB) is occupied).

2.1. D2D UEs Distribution and Receiver SINR

The signal-to-interference-plus-noise-ratio (SINR) at a receiver UE j' , that forms one of the many relay UEs in the D2D multi-hop link. The aggregated interference power at a receiver arises from two sources: (1) co-frequency D2D transmissions in the same BSs; (2) the transmission on CC links from all the BSs, I_{BS} . Therefore, for a relay UE that is of distance $r_{o,j'}$ from the nearest BS, the received SINR γ between any D2D relay j and j' is:

$$\gamma(r_{o,j'}) = \frac{H_{j,j'} P_{\text{D2D}} \lambda_{\text{D2D}} r_{j,j'}^{-\alpha}}{W + I_{\text{BS}}(r_{o,j'}) + \sum_{\substack{i \in \Phi \\ i \neq j}} H_{i,j'} P_{\text{D2D}} \lambda_{\text{D2D}} r_{i,j'}^{-\alpha}}, \quad (1)$$

where $I_{\text{BS}}(r_{o,j'})$ is the total interference from all BSs. The average interference power from the second nearest BS to further BS is [20]:

$$I_{\text{BS}}^{2nd} = \left[\frac{\pi \Lambda_{\text{BS}} \Xi(r_{o,j'}, \Psi, 4)}{2\sqrt{1/P_{\text{BS}} \lambda_{\text{BS}} \text{erfc}^{-1}(0.5)}} \right]^2, \quad (2)$$

so the total BS interference is comprised of the interference from the nearest BS that is of distance $r_{o,j'}$ away, and other further BSs.

$$I_{\text{BS}} = P_{\text{BS}} \lambda_{\text{BS}} r_{o,j'}^{-\alpha} + \left[\frac{\pi \Lambda_{\text{BS}} \Xi(r_{o,j'}, \Psi, 4)}{2\sqrt{1/P_{\text{BS}} \lambda_{\text{BS}} \text{erfc}^{-1}(0.5)}} \right]^2. \quad (3)$$

where $\Xi(r_{o,j'}, \Psi, 4) = \arctan(\Psi) - \arctan(r_{o,j'})$. The parameters for the above equations are as follows: W is the AWGN power, H is the fading gain, P is the transmission power, Λ is the density of the transmitters, λ is the frequency dependent pathloss constant, $r_{j,j'}$ is the distance between the transmitter and receiver D2D UEs, Ψ is the radius of the network coverage area for which an accurate BS density Λ can be determined [20], and α is the pathloss distance exponent. Typically, the aggregate interference power is significantly higher than the additive noise power W , and one can be assumed that the noise power is negligible. The full list of symbols used is given in Table 1.

3. Routing Strategies

3.1. Shortest-Path-Routing (SPR) Algorithm

SPR is a greedy algorithm, whereby each UE only makes routing decisions based on maximising its own performance with only local information. In greedy SPR, in order to make routing decisions,

Table 1 Symbol Notation

<i>Symbol</i>	<i>Definition</i>	<i>Parameter</i>	<i>Value</i>
γ	link SINR	Bandwidth	20 MHz
m	source D2D UE	Transmit Frequency	2.1 GHz DL
m'	destination D2D UE	macro-BS Number	19
j	Relay D2D UEs	CC UE Number/BS	120
o	nearest BS	D2D UE Number/BS	150
H	fading gain	Environment	Ottawa City
W	AWGN power	Propagation Model	3GPP UMi [21]
λ	pathloss constant	UE Distribution	PPP
P_{BS}	BS transmission power	ξ	-6 dB
P_{D2D}	D2D transmission power	AWGN Power	-132 dBm
ξ	SINR threshold	BS Antenna Height	45 m
R	max. D2D trans. distance	D2D User Height	1.5 m
$r_{j,j'}$	average hop distance	P_{BS}	40 W
$r_{j,j'}^{SPR}$	average hop distance for SPR	P_{D2D}	0.1 W
$r_{j,j'}^{IAR(i)}$	average hop distance for IAR	Λ_{D2D}	400/km ²
$K_{SPR,IAR}$	number of hops	Wall Loss	20 dB
R_{BS}	BS coverage range	Traffic Model	full buffer
Ψ	Macro-BSs coverage size	Multi-path Fading	Rayleigh
Λ_{D2D}	available D2D density	Fading Variance	6 dB
Λ'_{D2D}	co-frequency D2D density	Macro-BSs coverage	1650 m

it is required that each D2D UE knows its own location through its Global Position System (GPS) or other wireless localisation means (e.g., wireless fingerprinting). The SPR algorithm operates in the following manner:

1. The source UE m requests communication with a destination UE m' through standard authentication via the network. The serving BS authorises D2D communications and provides the location of destination UE m' to the source UE m , which is then used for route selection.
2. If destination m' is not in range of source m , UE m broadcasts a relay request and the request is received by neighbouring UEs in its communication range R , where R is the maximum distance for which reliable data transmission can take place. Available relay UEs will send back an acknowledgement to m .
3. UE m sends the data packet to the relay UE j that is the closest to the destination UE m' . The pseudo code is as follows: let Γ_K be the total set of available relay UEs j' at hop sequence $K = \{1, 2, 3, \dots, k\}$, and $r_{m,j'} \in L_k$ be the set of the distances between the potential forwarding UEs and m' .

While The communication data has not reached m'

1 Calculate distance L_k between Γ_k and UE m' ;

2 Find the UE j' with distance $\min L_k$;

3 Transmit the data to UE j' ;

End While

In the event that the D2D multi-hop process fails, the assisting BS will take over the communications and establish a standard CC link between the last successful relay UE and the destination UE. The BS assistance contains three main functions at each hop: (1) register the D2D UEs' identification (ID) and the D2D UE link layer identifier, (2) authorise the D2D UEs proximity discovery whereby the open discovery technology is used (in open discovery, the UEs can be detected by any other UE in its proximity [22]), and (3) provide the destination UE location to the relay UEs.

Fig. 1(b) illustrates the SPR algorithm between m and m' , where the solid line (in blue) shows the D2D multi-hop path, which can be approximately modelled by a straight line (accurate for high UE densities). Fig. 1(a) shows a D2D UEs, its maximum coverage range R , and how it selects a new relay UE j to forward the message to. The selection of D2D relay UE is dynamic and real-time when the UE finished the relaying it would be released from the D2D communication link. Furthermore, the relay UE can modify the routing path according to the periodically signal from the BS.

3.2. Interference-Aware-Routing (IAR) Algorithm

The idea behind IAR is to reduce the cross-tier interference from the BS to the D2D links. In the DL channel, the main interference is from the nearest BS (dominant inter) and co-frequency D2D transmissions (intra). In order to minimise the interference from the BS, the multi-hop route attempts to travel along the cell-edge of the coverage area. This is shown in Fig. 1(b) with a circular coverage area for illustration purposes. For a pair of arbitrarily located source and destination UEs, there are three individual stages to the IAR algorithm, and each stage uses the previously described SPR algorithm to accomplish it:

1. *Stage 1 Escape*: multi-hop from source UE m to the closest UE to the cell-edge, this is achieved using SPR;
2. *Stage 2 Migrate*: multi-hop from one cell-edge UE to another cell-edge UE that is closest to the destination m' ;
3. *Stage 3 Return*: multi-hop from the cell-edge UE to the destination UE m' , this is achieved using SPR.

If there are no D2D UEs that satisfied the condition of IAR, the routing will switch to the previously mentioned SPR scheme and relay directly to the destination UE. In most cases, the IAR algorithm increases the path length significantly in comparison to the SPR algorithm, but the advantage is that the interference from the BS can be reduced significantly due to the increased distance from the nearest BS.

4. Quality-of-Service (QoS) Performance

The QoS performance metrics associated with D2D are primarily related to outage probability, as the data is usually relayed several times - leading to a higher than normal probability of outage. We will also examine the capacity of the overall relay channel, as a secondary QoS. For the outage probability, we define the corresponding success probability as the probability of receiving the data bearing signal at the receiver. In order to do this, the SINR at each hop stage needs to be greater than a data communication threshold ξ .

$$f_{\epsilon, r_{m,m'}}(\epsilon) = \begin{cases} \sum_{n=0}^{\infty} G(n) 2n(r_{m,m'} - \epsilon) \arccos\left(1 + \frac{\epsilon^2 - R^2}{2r_{m,m'} - (r_{m,m'} - \epsilon)}\right) \\ \quad \times \left[\frac{1}{2} \sqrt{4R^2 r_{m,m'}^2 - (R^2 - \epsilon^2 + 2r_{m,m'} \epsilon)^2} \right. \\ \quad \left. - (r_{m,m'} - \epsilon)^2 \arccos\left(1 + \frac{\epsilon^2 - R^2}{2r_{m,m'} - (r_{m,m'} - \epsilon)}\right) \right. \\ \quad \left. + R^2 \arcsin\left(\frac{R^2 - \epsilon^2 + 2r_{m,m'} \epsilon}{2lR}\right) \right]^{n-1} & 0 \leq \epsilon \leq R \\ 0 & \text{elsewhere,} \end{cases} \quad (5)$$

4.1. Average Hop Distance

4.1.1. Maximum Transmission Distance: In order to characterise the success probability performance of the SPR and IAR algorithms, it is necessarily first to determine the average hop distance of each scheme. As shown in Fig. 1(a), each UE is capable of transmitting a signal of up to an average range R , which covers an area $A = \pi R^2$. For each hop, the D2D UE within the range R closest to the destination is selected as a relay UE for the next hop, the hop distance is ϵ . For the QoS requirement of the data communication, the minimum SINR required is ξ . Therefore, using Eq. (1) to find the maximum value of $r_{j,j'}$, the maximum of D2D transmission distance for a single hop is (see Section 7.1):

$$R = \arg \max \{r_{j,j'} | \gamma(r_{o,j'}) \geq \xi\} = \left[\xi \frac{I_{BS}(r_{o,j'})}{P_{D2D} \lambda_{D2D}} + \xi \sum_{\substack{i \in \Phi \\ i \neq j}} r_{i,j'}^{-\alpha} \right]^{-1/\alpha}. \quad (4)$$

4.1.2. Average Hop Distance for Single Hop: Given the maximum hop distance, then the average hop distance can be found. As mentioned before, the assumption was made that the D2D UEs are randomly and uniformly distributed. Let the Euclidean distance between source UE m and destination UE m' be $r_{m,m'}$. The probability density function (PDF) of the maximum single hop distance ϵ presented as Eq. 5 is given by [23]. The mean hop distance for each single hop under these assumptions is therefore ¹:

$$r_{j,j'} = \mathbb{E}[\epsilon] = \int_0^{R(r_{o,j'})} \epsilon f_{\epsilon, r_{m,m'}}(\epsilon) d\epsilon, \quad (6)$$

subject to the maximum hop distance R constraint given in Eq.(4).

4.2. Success Probability for Single Hop D2D

The assumption is made that the interference distances are always greater than the D2D transmission distance. This is reasonable given that the BS is farther compared with the distance of a D2D hop, and that the interfered D2Ds are located in neighbouring BSs. The success probability at the

¹There is an assumption that there are minor interference differences in the D2D relay UEs at different locations because the interference in the DL channel is from a BS, the resulting interference differences in a small spatial circle are small.

k -th hop is defined as (see Section 7.2).

$$\mathbb{P}_k = \mathbb{P}[\gamma > \xi]$$

$$= \exp \left\{ -\beta_{\text{D2D}} r_{j,j'}^\alpha P_{\text{BS}} \lambda_{\text{BS}} r_{o,j'}^{-\alpha} - \frac{P_{\text{BS}} \lambda_{\text{BS}}}{P_{\text{D2D}} \lambda_{\text{D2D}}} r_{j,j'}^\alpha \left[\frac{\pi \Lambda_{\text{BS}} \Xi(r_{o,j'}, \Psi, 4)}{2\text{erfc}^{-1}(0.5)} \right]^2 - \Lambda'_{\text{D2D}} \pi r_{i,j'}^2 Q(\xi, \alpha) \right\}, \quad (7)$$

where $\beta_{\text{D2D}} = 1/P_{\text{D2D}} \lambda_{\text{D2D}}$. The parameter $\Lambda'_{\text{D2D}} = N'_{\text{D2D}}/\pi R_{\text{BS}}^2$ is the density of co-frequency D2D UEs and should not be confused with Λ_{D2D} , which is the density of potential D2D UEs in existence. The parameter $r_{i,j'}$ is the distance of a hop and ξ is the minimum data connectivity SINR threshold for realistic modulation and coding schemes (MCS). The $Q(\cdot)$ function is given by:

$$\begin{aligned} Q(\xi, \alpha) &= \int_{\xi^{-2/\alpha}}^{+\infty} \frac{\xi^{2/\alpha}}{1+u^{\alpha/2}} du \\ &= \sqrt{\xi} \arctan(\sqrt{\xi}) \quad \text{for } \alpha = 4. \end{aligned} \quad (8)$$

4.3. Success Probability for multi-hop SPR Scheme

The success probability calculation is given in Algorithm 1 Success Probability.

Algorithm 1 Success Probability

```

1: procedure PROBABILITY  $\mathbb{P}_{\text{SPR}}(r_{o,m}, r_{o,m'}, \theta, \xi)$ 
2:   if  $\gamma(r_{o,m}) \geq \xi$  then % The 1st hop SINR requirement
3:     The distance to the BS is assumed  $r_{o,j'} = r_{o,j}$ 
4:     Max. range  $R(r_{o,m})$  from (4)
5:     The hop forward distance  $r_{j,j'}$  from (6)
6:     The probability  $\mathbb{P}_{\text{SPR},1}$  from (8) and (10)
7:     From the second hop to the  $k$ -th hop
8:     while destination node  $m'$  not reached do
9:       The distance to the BS  $r_{o,j'}(k)$  from (9)
10:      Max. range  $R(r_{o,j'}(k))$  from (4)
11:      The hop forward distance  $r_{j,j'}^{\text{SPR}}(k)$  from (9)
12:      The probability  $\mathbb{P}_{\text{SPR},k}$  from (8) and (10)
13:    end while
14:  end if
15:   $\mathbb{P}_{\text{SPR}} = \prod_{k=1}^k \mathbb{P}_{\text{SPR},k}$ 
16: end procedure

```

For the scenario of SPR shown in Fig. 1(b), the average distance of each hop $r_{j,j'}^{\text{SPR}}$ is defined in

Eq.4 and Eq.6 as:

$$\begin{aligned}
r_{j,j'}^{\text{SPR}}(k) &= \int_0^{R[r_{o,j'}(k)]} \varepsilon f_{\varepsilon, r_{m,m'}}(\varepsilon) d\varepsilon \\
r_{o,j'}(k) &= \sqrt{r_{o,m}^2 + \left(\sum(.)\right)^2 - 2r_{o,m} \sum(.) \cos \theta'} \\
\text{where } \sum(.) &= \sum_{i=1}^{K_{\text{SPR}}} r_{j,j'}^{\text{SPR}}(k-1) \\
\text{and } \cos \theta' &= \frac{r_{o,m}^2 + r_{m,m'}^2 - r_{o,m'}^2}{2r_{o,m}r_{m,m'}},
\end{aligned} \tag{9}$$

where the hop distance is relatively short such that the assumption is $r_{o,j'} \approx r_{o,j}$, so $r_{o,j'} = r_{o,m}$.

From Eq. 7, the success communication probability for the multi-hop SPR at the k -th hop is:

$$\begin{aligned}
\mathbb{P}_{\text{SPR},k} &= \exp \left\{ - \left(\frac{r_{j,j'}^{\text{SPR}}(k)}{r_{o,j'}(k)} \right)^\alpha \left(\frac{P_{\text{BS}}}{P_{\text{D2D}}} \right) \right. \\
&\quad \left. - \frac{P_{\text{BS}}}{P_{\text{D2D}}} [r_{j,j'}^{\text{SPR}}(k)]^\alpha \left[\frac{\pi \Lambda_{\text{BS}} \Xi(r_{o,j'}(k), \Psi, 4)}{2\text{erfc}^{-1}(0.5)} \right]^2 - \left(\frac{r_{j,j'}^{\text{SPR}}(k)}{R_{\text{BS}}} \right)^2 N'_{\text{D2D}} Q(\xi, \alpha) \right\},
\end{aligned} \tag{10}$$

where the D2D shares the band link with the BS, so that the frequency dependent pathloss constant $\lambda_{\text{BS}} = \lambda_{\text{D2D}}$. It can be seen that the success probability is a function of the distance from the closest BS to the relay UE j ($r_{o,j'}$).

When there is a high density of D2D UEs available, the resulting multi-hop path is approximated a straight line between m and m' . So the total hop distance is the Euclidean distance between m and m' : $r_{m,m'} = \sqrt{r_{o,m}^2 + r_{o,m'}^2 - 2r_{o,m}r_{o,m'} \cos \theta}$. Therefore the total number of hops is K_{SPR} satisfied:

$$r_{m,m'} = \sum_{k=1}^{K_{\text{SPR}}} r_{j,j'}^{\text{SPR}}(k). \tag{11}$$

Given that the successful probability of a multi-hop transmission is the product of the success at each link, the overall success probability is therefore:

$$\mathbb{P}_{\text{SPR}} = \prod_{k=1}^{K_{\text{SPR}}} \mathbb{P}_{\text{SPR},k}. \tag{12}$$

The results in Fig. 2 for different values of θ show the theoretical success probability of D2D UEs at any location in a BS using the multi-hop SPR algorithm. As the angle θ decreases, the success probability increases significantly. For large angles (approaching π), the SPR route will inevitably cross near the BS, incurring greater mutual interference. In terms of the distance from the BS to the source or destination UEs, the greater the distance the stronger the success probability, which means that D2D communications should be avoided close to the BS.

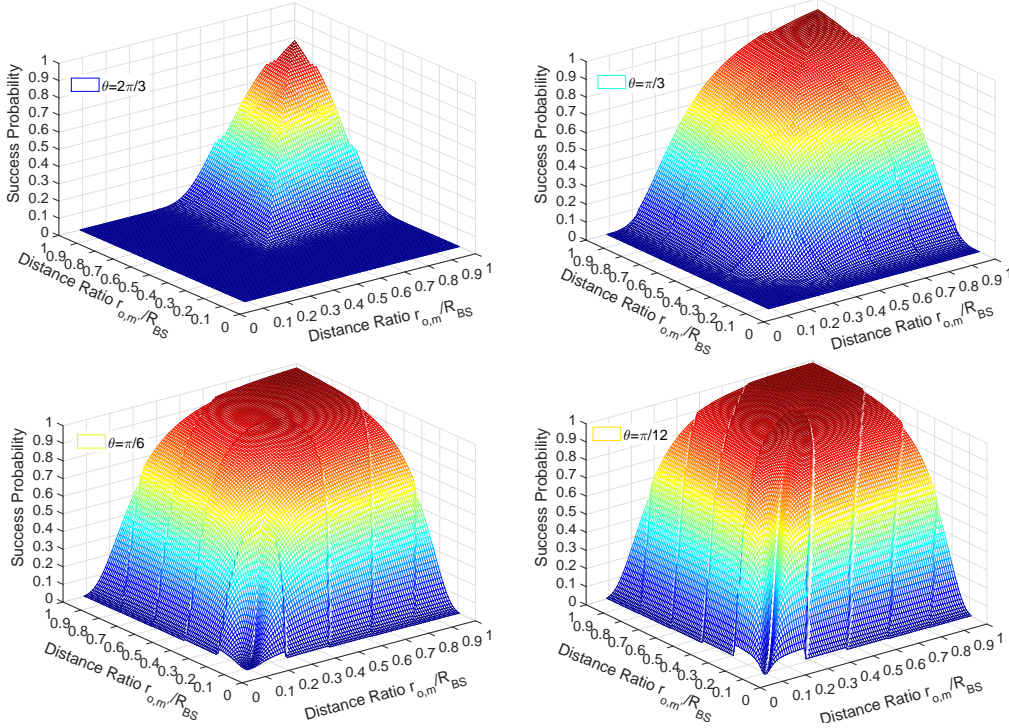


Fig. 2. The success probability of SPR D2D at different locations: x and y axes are the distance ratio scale of $r_{o,m}$ and $r_{o,m'}$ to R_{BS} .

4.4. Success Probability for IAR Scheme

As mentioned previously, there are three main *stages* to the IAR algorithm: (1) Escape, (2) Migrate and (3) Return. Each *stage* of the IAR utilizes the aforementioned SPR algorithm, and the success probability for each IAR stage can be derived from Eq. 10 and Eq. 12.

4.4.1. Stage 1: Escape: For the first multi-hop stage (IAR(1)), the source UE m attempts to use SPR to transmit to the nearest point on the cell-edge, so the total routing distance for this stage is $(R_{BS} - r_{o,m})$. At the k -th hop, the distance from the BS to the relay UE is: $r_{o,j'}(k) = r_{o,m} + \sum_2^k r_{j,j'}^{IAR(1)}(k-1)$, where the average hop distance for each single k -th hop is $r_{j,j'}^{IAR(1)}(k) = \int_0^{R[r_{o,j'}(k)]} \varepsilon f_{\varepsilon, r_{m,m'}}(\varepsilon) d\varepsilon$ and $r_{o,j'}(1) = r_{o,m}$. From Eq. 10, the probability of success at the k -th hop in this stage is:

$$\mathbb{P}_{IAR(1),k} = \exp \left\{ - \left(\frac{r_{j,j'}^{IAR(1)}(k)}{r_{o,m} + \sum_2^k r_{j,j'}^{IAR(1)}(k-1)} \right)^\alpha \left(\frac{P_{BS}}{P_{D2D}} \right) - \frac{P_{BS}}{P_{D2D}} [r_{j,j'}^{IAR(1)}(k)]^\alpha \left[\frac{\pi \Lambda_{BS} \Xi(r_{o,m} + r_{j,j'}^{IAR(1)}(k), \Psi, 4)}{2 \operatorname{erfc}^{-1}(0.5)} \right]^2 - \left(\frac{r_{j,j'}^{IAR(1)}(k)}{R_{BS}} \right)^2 N'_{D2D} Q(\xi, \alpha) \right\}, \quad (13)$$

The total number of hops in the first stage is $K_{IAR(1)}$, where $R_{BS} - r_{o,m} = \sum_{k=1}^{K_{IAR(1)}} r_{j,j'}^{IAR(1)}(k)$. Therefore the success probability for the entire *Escape* stage is $\mathbb{P}_{IAR(1)} \approx \prod_{k=1}^{K_{IAR(1)}} \mathbb{P}_{IAR(1),k}$.

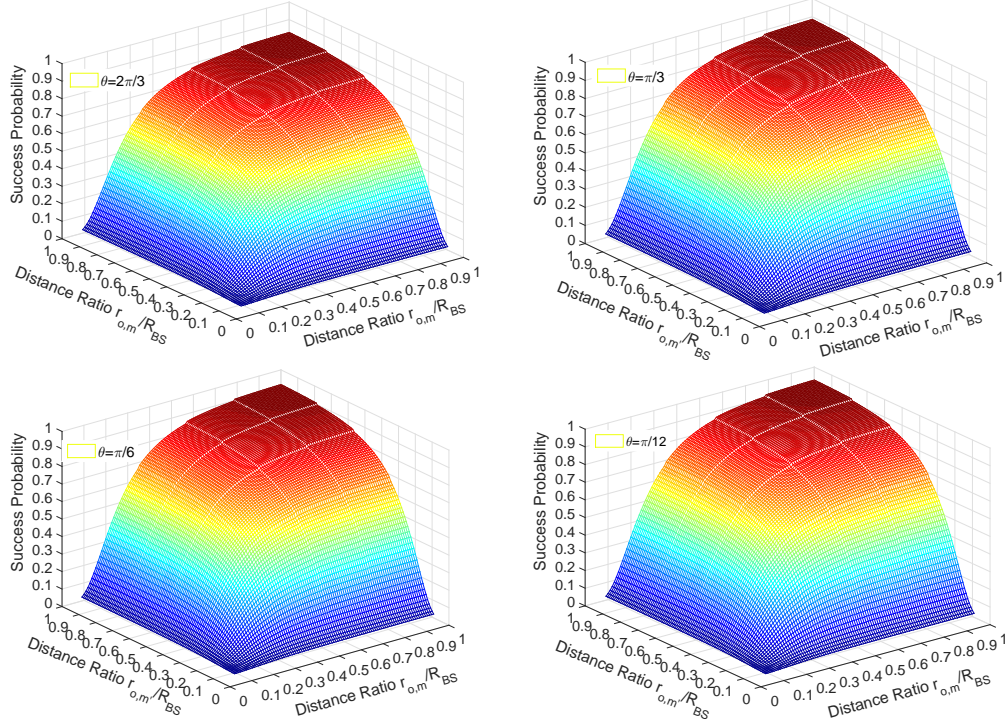


Fig. 3. The success probability of IAR D2D at different locations: x and y axes are the distance ratio scale of $r_{o,m}$ and $r_{o,m'}$ to R_{BS} .

4.4.2. Stage 2: Migrate: For the second multi-hop stage (IAR(2)), the route is from the cell-edge UE closest to source to another cell-edge UE that is closest to the destination. At any given point along the route, the distance from the BS to any of the relay UEs is approximately R_{BS} (i.e. the cell coverage area is modelled as a circle). The total hops distance for the stage is $\theta \times R_{BS}$. Therefore, the average hop distance through the stage is $r_{j,j'}^{IAR(2)}(k) = \int_0^{R(R_{BS})} \varepsilon f_{\varepsilon, r_{m,m'}}(\varepsilon) d\varepsilon$. From Eq. 10, the probability of success for each hop is:

$$\begin{aligned} \mathbb{P}_{IAR(2),k} = \exp \left\{ - \left(\frac{r_{j,j'}^{IAR(2)}}{\theta \times R_{BS}} \right)^\alpha \left(\frac{P_{BS}}{P_{D2D}} \right) \right. \\ \left. - \frac{P_{BS}}{P_{D2D}} [r_{j,j'}^{IAR(2)}]^\alpha \left(\frac{\pi \Lambda_{BS} \Xi(\theta \times R_{BS}, \Psi, 4)}{2 \operatorname{erfc}^{-1}(0.5)} \right)^2 - \left(\frac{r_{j,j'}^{IAR(2)}}{R_{BS}} \right)^2 N'_{D2D} Q(\xi, \alpha) \right\}. \end{aligned} \quad (14)$$

The total number of hops in the second stage in the IAR algorithm is $K_{IAR(2)} = (\theta \times R_{BS}) / r_{j,j'}^{IAR(2)}$. Therefore the success probability of the entire *Migrate* stage is $\mathbb{P}_{IAR(2)} \approx \prod_{k=1}^{K_{IAR(2)}} \mathbb{P}_{IAR(2),k}$.

4.4.3. Stage 3: Return: For the third multi-hop stage, it is a multi-hop from the boundary relay UE back to the destination UE so the distance from BS to the k -th hop UE is: $r_{o,j'}(k) = R_{BS} - \sum_{i=2}^k r_{j,j'}^{IAR(3)}(i-1)$, where the hop forward distance for each single hop through the entire IAR *Escape* stage is $r_{j,j'}^{IAR(3)}(k) = \int_0^{R(r_{o,j'}(k))} \varepsilon f_{\varepsilon, r_{m,m'}}(\varepsilon) d\varepsilon$ and $r_{o,j'}(1) = R_{BS}$ and $r_{o,j'} = R_{BS}$. The total UE hops distance for this stage is $R_{BS} - r_{o,m'}$. From Eq. 10, the probability of success for the

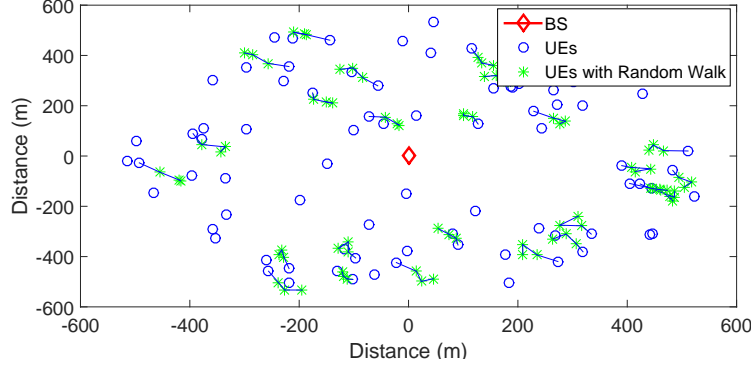


Fig. 4. A snapshot of the simulation setup consisting of D2D UEs moving inside the coverage area of a single BS.

k -th hop is:

$$\mathbb{P}_{\text{IAR}(3),k} = \exp \left\{ - \left(\frac{r_{j,j'}^{\text{IAR}(3)}(k)}{R_{\text{BS}} - \sum_{k=2}^k r_{j,j'}^{\text{IAR}(3)}(k-1)} \right)^\alpha \times \left(\frac{P_{\text{BS}}}{P_{\text{D2D}}} \right) - \frac{P_{\text{BS}}}{P_{\text{D2D}}} [r_{j,j'}^{\text{IAR}(3)}(k)]^\alpha \right. \\ \left. \times \left[\frac{\pi \Lambda_{\text{BS}} \Xi(R_{\text{BS}} - \sum_{k=2}^k r_{j,j'}^{\text{IAR}(3)}(k-1), \Psi, 4)}{2\text{erfc}^{-1}(0.5)} \right]^2 - \left(\frac{r_{j,j'}^{\text{IAR}(3)}(k)}{R_{\text{BS}}} \right)^2 N'_{\text{D2D}} Q(\xi, \alpha) \right\}, \quad (15)$$

The total number of hops in the third stage in the IAR algorithm is $K_{\text{IAR}(3)}$ where $R_{\text{BS}} - r_{o,m'} = \sum_{k=1}^{K_{\text{IAR}(3)}} r_{j,j'}^{\text{IAR}(3)}(k)$. Therefore, success probability for the entire stage *Return* is $\mathbb{P}_{\text{IAR}(3)} \approx \prod_{k=1}^{K_{\text{IAR}(3)}} \mathbb{P}_{\text{IAR}(3),k}$.

4.4.4. Synthesis: The overall success probability from source D2D user to destination D2D user by IAR is:

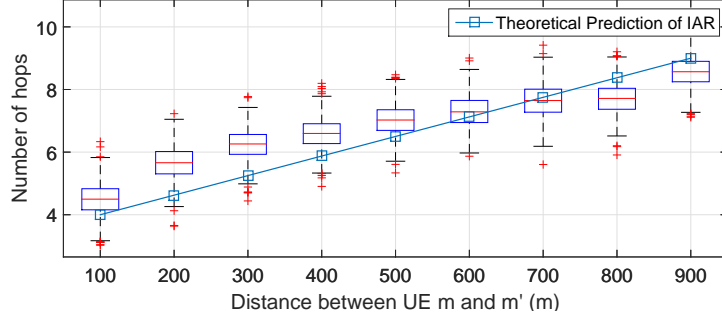
$$\mathbb{P}_{\text{IAR}} = \prod_{i=1}^3 \mathbb{P}_{\text{IAR}(i)}, \quad (16)$$

and the total number of hops is: $K_{\text{IAR}} = \sum_{i=1}^3 K_{\text{IAR}(i)}$.

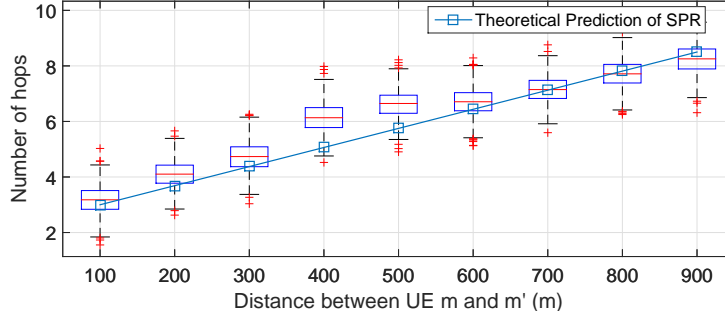
Fig. 3 shows the theoretical success probability of D2D UEs in different locations employing the IAR algorithm. Compared with the SPR algorithm shown previously in Fig. 2, the angle θ for IAR is not a significant effect parameter, whereas the distances of the source and destination UEs to the BS are. Generally the IAR has better performance of success probability than SPR for D2D routes that are of longer distance and are further away from the BS. In terms of distance from the BS of the source or destination UEs, the greater the distance the stronger the success probability, which means that D2D communications should be avoided close to the BS.

5. Results and Analysis

We now consider a specific urban terrain, which is covered by 19 macro-BSs in Voronoi configuration with a central macro-BS as shown in Fig. 4, where a number of D2D UEs are located. A



(a) The theoretical number of hops for IAR compared with box plot simulation results.



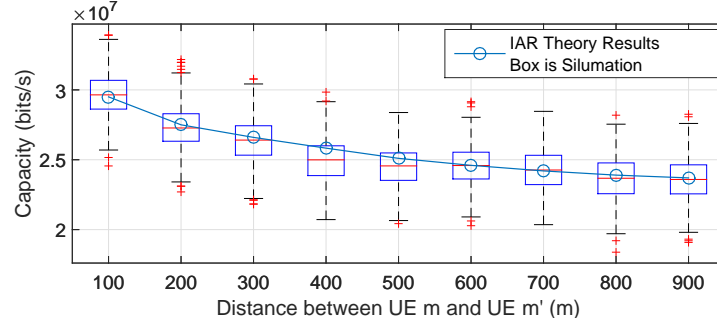
(b) The theoretical number of hops for SPR compared with box plot simulation results.

Fig. 5. The theoretical number of hops for IAR and SPR routing schemes compared with the box plot plot of their simulation results.

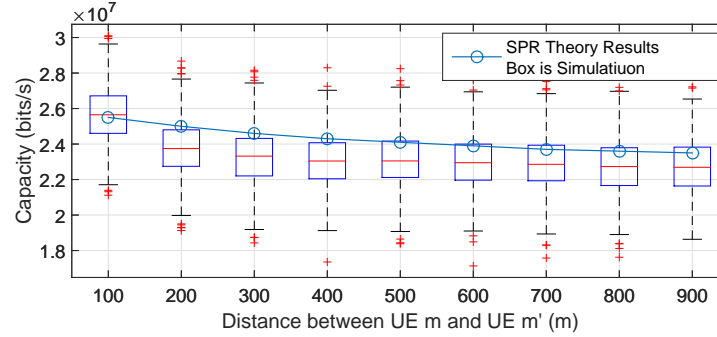
Random Walk model is added to the simulation to model user mobility (each circle represents a new position of the user with connecting lines to show the movement trace). Within that set of UEs, a source and destination UEs are randomly selected. The specific system and propagation parameters are in accordance to Table 1.

5.1. Number of Hops

The detailed performance of the D2D underlay tier is now considered. The number of hops of each scheme is an important indication of relay UE utilization level. The more hops each scheme uses, the greater the chance of data loss, privacy violation, and the less efficient the scheme is in terms of hardware utilization. Fig. 5 shows the number of hops for the two respective schemes, as a function of the Euclidean distance between source and destination UEs. The first set of observations is that the number of hops is increasing *linearly* with the distance for both SPR and IAR. Whilst for the same distance between m and m' the average number of hops for IAR is greater than SPR, the difference becomes smaller for longer distances between UEs. That means the advantage of IAR at long distances is significant, as it can dramatically reduce interference between D2D and CC UE channels. The second set of observations is that the theory matches the simulation data well. The accuracy diminishes for distances below 400 m, because the noise due to random UE placements causes the routing path to resemble an arc as opposed to a straight line.



(a) The theoretical capacity for IAR compared with box plot simulation results.



(b) The theoretical capacity for SPR compared with box plot simulation results.

Fig. 6. The comparative theoretical capacity for IAR and SPR routing schemes (box plot of their simulation results).

5.2. Network Capacity

For the Shannon theory, the network capacity at each hop link related to SINR, which is:

$$\mathcal{C}_k = B \log_2 (1 + r_{o,j'}) , \quad (17)$$

where \mathcal{C} is the network capacity at k -th hop, and B is the network bandwidth. By using the SINR values found previously for SPR and IAR schemes, one can find the associated capacity values.

Fig. 6 shows the theoretical predicted capacity of the D2D channel comparing with a box plot of the simulation results. The results show that D2D multi-hop links in coexistence with CC interference can achieve the link capacity from 19 Mbits/s to 33 Mbits/s depends on the different D2D UE location. The IAR is able to consistently achieve a superior throughput (10%) in comparison with SPR, because it attempts to reduce interference from the macro-BS when planning its longer route. In terms of the capacity of the CC UEs, the CC capacity performance is dropped from 53.9 Mbits/s to 52.6 Mbits/s when in coexistence with SPR and dropped to 52.9 Mbits/s when in coexistence with IAR. SPR and IAR D2D only degrade the CC capacity performances by 2.4% and 1.8% respectively. The capacity gain by offloading to D2D is approximately 43% for SPR and 51% for IAR. This is a significant improvement over cellular network and no significant increase in operational expenditures (i.e., backhaul infrastructure or rental costs) is incurred [24]. The sacrifice IAR makes to incur a longer route and involving more participating UEs, now be examined.

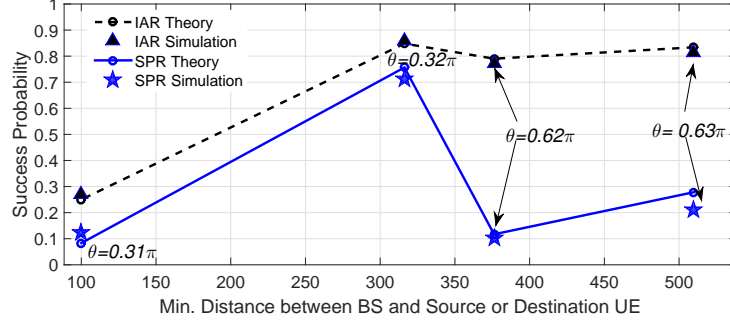


Fig. 7. Compression of success probability with theory (line) and simulation (symbol) as a function of the minimum distance from BS to one of the source and destination UEs: $\min[r_{o,m}, r_{o,m'}]$.

5.3. Communication Success Probability

The communication success probability as a function of the minimum distance from BS to one of the source and destination UEs is now considered, and the effect of angle θ is also observed. Fig. 7 shows the simulation results (symbols) and theory (lines), and there is good agreement between the theory and simulation results.

The first observation is that both the SPR and IAR can achieve a high success probability ($\geq 70\%$) if certain spatial conditions are met. For SPR, the spatial conditions are: (1) the source or destination UE is far from the closest BS, and (2) there is a small incident angle θ in order to avoid the possibility of routing close to the closest interfering BS. For IAR, there is only one condition and that is the source or destination UE is far from the closest BS. If both of these scenarios are met, then the performance of SPR and IAR are approximately equal and that makes intuitive sense as the route is also similar. The angle θ between two UEs does not affect IAR communications, as shown in Fig. 7. For SPR, the angle can affect the success probability dramatically, as shown in Fig. 7. This is consistent with results from earlier in the paper (see Fig. 2 and Fig. 3). This is primarily because for SPR, the interference from the BS will be excessive, whereas for IAR, the routing path will always be at maximum distance from the BS, minimizing interference.

It was found that the IAR scheme can improve both the D2D transmission success by from 14% to 18%, but will incur up to 20% more UEs to participate, which can incur privacy concerns. The privacy issue is beyond the scope of this paper.

5.4. Operational Zones and Offloaded Traffic Volume

We guarantee QoS through operation zones. These are spatial zones, whereby only one type of transmission is permitted to guarantee QoS for other users in the network. In Fig. 8, we show D2D operational zones for different transmission strategies. The operation zone is closely related to the base station coverage area, whereby the zones have a sectorized shape and are defined with an angle of $\angle mom'$ and the distance ratio of the D2D UEs to the BS. For example, in zone 5, the distance of m and m' both bigger than the $0.45R_{BS}$ and the $\angle mom' < \pi/2$. So the IAR is selected as a routing algorithm. The full list of operation zone scenarios are as follows:

- **No D2D:** when the source or destination UEs are located within less than 45% of the cell radius from the BS, which is under the condition that the success probability is greater than 55% of IAR at angle θ is from 0 to π and of SPR angle θ is from 0 to $\pi/4$, no D2D routing should take place and all traffic should be handled by the BS as CC links.

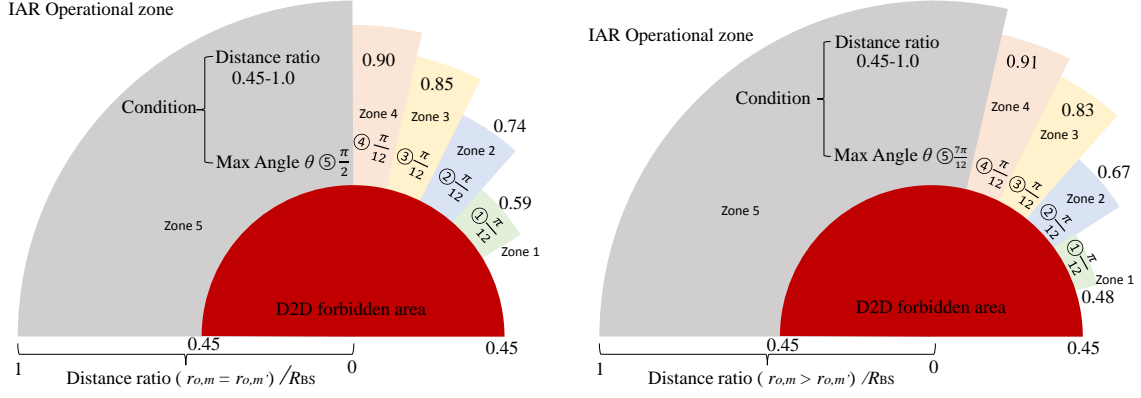


Fig. 8. The interference routing algorithm in a cell with the distance ratio scale of $r_{o,m}$ and $r_{o,m'}$ to R_{BS} .

- **IAR:** when the source and destination UEs are located far apart such that the angle is greater than $\pi/2$ with the distance ratio $r_{o,m}/R_{BS} = r_{o,m'}/R_{BS}$ for far from BS or the angle is greater than $5\pi/12$ with the distance ratio $r_{o,m}/R_{BS} > r_{o,m'}/R_{BS}$, and greater than $\pi/4$ for medium distance from BS; IAR should be used as a preference algorithm. If the UEs are any closer then SPR may be preferable.
- **SPR:** when the source and destination UEs are located in close proximity such that the angle $0 \leq \theta \leq \pi/6$; SPR should be used as a preference D2D routing algorithm. If the UEs are any further then IAR may be preferable.

In summary, for the IAR algorithm, it is generally preferable if the source and destination UEs are far from the BS and the separation distance or angle is not less than $\pi/6$. The effect of the angle is not significant beyond this basic constraint. More than 70% of UEs in a cell fit this category. For SPR, the effect of angle is paramount, especially when the distance between the UEs is not small. Hence, SPR is only feasible for D2D communications between relatively nearby UEs, or those that already sit on the edge of the BS's coverage area. By knowing the source and destination UEs' locations, the appropriate routing algorithm can be devised as an operational zone. The UEs are distributed as a Poisson distribution in the network, the total traffic rate offloaded from the cellular network is the ratio of the area of operation zone to the area of the BS. The maximum of the offload traffic from the BS is $O_{SPR} = \frac{A_{SPR}}{A_{BS}}$ for SPR and $O_{IAR} = \frac{A_{IAR}}{A_{BS}}$ for IAR. The parameter A_{IAR} is the operation area for the IAR and A_{SPR} is the operation area for the SPR, and A_{BS} is the area size of BS. Therefore, the maximum offload traffic ratio from BS is 79.75% and the ratio for IAR is 49.985% and for SPR is 29.765%.

6. Conclusions

Device-to-device (D2D) communications can improve overall network capacity and is beneficial in spectrum scarce environments. However, D2D transmissions over a significant distance requires several relay hops and dynamic routing that minimises cross-tier interference is not well understood. Traditional greedy-based algorithms such as Shortest-Path-Routing (SPR) can cause high levels of interference and diminish both D2D and conventional cellular (CC) performance. In this paper, we analyse a proposed Interference-Aware-Routing (IAR), whereby the spatial routing path

is selected to minimise cross-tier interference.

Several key discoveries have been presented in this paper. Firstly, a longer routing path that minimises cross-tier interference can achieve a superior performance compared to the intuitive shortest path route. We also employ spatial operation envelopes to define where IAR and SPR D2D algorithms should be utilised and where D2D should be avoided all together. This is our second discovery, which is that there are clear geometric regions in the macro-cell coverage area that determine the D2D operations. In terms of performance metrics, it was found that the negative effect of D2D routing on regular cellular communications (CC) is negligible (1% to 2% degradation), and D2D communications can improve the CC network capacity by 44% for the SPR and 50% for the IAR routing scheme. When considering the D2D tier in isolation, the improvement of IAR over SPR is approximately 10% in capacity and 14% in outage probability. This demonstrates that careful cross-tier interference avoidance can yield productive improvements both within the D2D transmissions, but also for the conventional cellular links. Furthermore, we employ dynamic selection between the different D2D routing algorithms and CC, enabling the network to offload 79.75% of the traffic volume from the assisting BS.

7. Appendices

7.1. The D2D UEs maximum transmission distance

As the minimum SINR required by QoS, data communication SINR threshold at the receiver D2D is the ξ , so the maximum transmission distance is:

$$\frac{H_{j,j'} P_{D2D} \lambda_{D2D} [R(r_{o,j'})]^{-\alpha}}{W + I_{BS}(r_{o,j'}) + \sum_{\substack{i \in \Phi \\ i \neq j}} H_{i,j'} P_{D2D} \lambda_{D2D} r_{i,j'}^{-\alpha}} \geq \xi, \quad (18)$$

where the $I_{BS}(r_{o,j'})$ is shown in Eq. 3. Without considering instantaneous fading and the Gaussian noise effects, the R is:

$$\begin{aligned} \frac{P_{D2D} \lambda_{D2D} [R(r_{o,j'})]^{-\alpha}}{I_{BS}(r_{o,j'}) + \sum_{\substack{i \in \Phi \\ i \neq j}} P_{D2D} \lambda_{D2D} r_{i,j'}^{-\alpha}} &\geq \xi, \\ [R(r_{o,j'})]^\alpha &\leq \frac{P_{D2D} \lambda_{D2D}}{\xi I_{BS}(r_{o,j'}) + \xi \sum_{\substack{i \in \Phi \\ i \neq j}} P_{D2D} \lambda_{D2D} r_{i,j'}^{-\alpha}} \end{aligned} \quad (19)$$

So the maximum transmission range is:

$$\begin{aligned}
\arg \max \{R(r_{o,j'})\} &= \left\{ \frac{P_{D2D} \lambda_{D2D}}{\xi I_{BS}(r_{o,j'}) + \xi \sum_{\substack{i \in \Phi \\ i \neq j}} P_{D2D} \lambda_{D2D} r_{i,j'}^{-\alpha}} \right\}^{1/\alpha} \\
&= \left\{ \frac{\xi I_{BS}(r_{o,j'}) + \xi \sum_{\substack{i \in \Phi \\ i \neq j}} P_{D2D} \lambda_{D2D} r_{i,j'}^{-\alpha}}{P_{D2D} \lambda_{D2D}} \right\}^{-1/\alpha} \\
&= \left[\xi \frac{I_{BS}(r_{o,j'})}{P_{D2D} \lambda_{D2D}} + \xi \sum_{\substack{i \in \Phi \\ i \neq j}} r_{i,j'}^{-\alpha} \right]^{-1/\alpha}.
\end{aligned} \tag{20}$$

7.2. Single hop Success communication probability

Success probability of the D2D transmission is defined $\mathbb{P}[\text{SINR} > \xi]$. Defining $g_{j,j'} = H_{j,j'} P_{D2D} \lambda_{D2D}$ and $I_{D2D}(r_{i,j'}, H_{i,j}) = \sum_{\substack{i \in \Phi \\ i \neq j}} H_{i,j'} P_{D2D} \lambda_{D2D} r_{i,j'}^{-\alpha}$, the probability is:

$$\begin{aligned}
\mathbb{P}_{\text{Success}} &= \mathbb{P} \left[\frac{g_{j,j'} r_{j,j'}^{-\alpha}}{I_{BS}(r_{o,j'}) + I_{D2D}(r_{i,j'}, H_{i,j})} > \xi \right] \\
&= \mathbb{P} \left\{ g_{j,j'} > r_{j,j'}^{\alpha} \left[I_{BS}(r_{o,j'}) + I_{D2D}(r_{i,j'}, H_{i,j}) \right] \right\} \\
&= \int_0^{+\infty} \int_{\zeta}^{+\infty} f_G(g) f_R(I_{D2D}|r_{i,j}) dg dI_{D2D},
\end{aligned} \tag{21}$$

where $\zeta = r_{j,j'}^{\alpha} (I_{BS}(r_{o,j'}) + I_{D2D}(r_{i,j'}, H_{i,j}))$. The multipath fading has a PDF of $f_G(g) \sim \exp(-\beta g)$ where $\beta_{D2D} = 1/P_{D2D} \lambda_{D2D}$ and $f_R(I_{D2D}|r_{i,j})$ is the joint interference distribution. Applying the fading distribution:

$$\begin{aligned}
\mathbb{P}_{\text{Success}} &= \exp \left[-\beta_{D2D} r_{j,j'}^{\alpha} I_{BS}(r_{o,j'}) \right] \int_0^{+\infty} f_R(I_{D2D}|r_{i,j}) e^{-\beta_{D2D} r_{j,j'}^{\alpha} I_{D2D}(r_{i,j'}, H_{i,j})} dI_{D2D} \\
&= \exp \left[-\beta_{D2D} r_{j,j'}^{\alpha} I_{BS}(r_{o,j'}) \right] \mathcal{L} \left(\beta_{D2D} r_{j,j'}^{\alpha} \right),
\end{aligned} \tag{22}$$

where $\mathcal{L}()$ is the Laplace transform of the interference term I_{D2D} .

The Laplace transform of the interference signal power by D2D UEs is:

$$\begin{aligned}
\mathcal{L}(\beta_{\text{D2D}} r_{i,j'}^\alpha) &= \int_{r_{i,j'}}^{+\infty} \int_0^{+\infty} \exp\left(-\sum_{\substack{i \in \Phi \\ i \neq j}} \beta_{\text{D2D}} r^\alpha g_i r_{i,j'}^{-\alpha}\right) f_G(g_i) f_R(r_{i,j'}) dg_i dr_{i,j'} \\
&= \int_{r_{i,j'}}^{+\infty} \int_0^{+\infty} \prod_{\substack{i \in \Phi \\ i \neq j}} \exp\left(-\beta_{\text{D2D}} r^\alpha g_i r_{i,j'}^{-\alpha}\right) f_G(g_i) f_R(r_{i,j'}) dg_i dr_{i,j'} \\
&= \exp\left[-\Lambda'_{\text{D2D}} \pi r_{i,j'}^2 Q(\xi, \alpha)\right],
\end{aligned} \tag{23}$$

where the D2D is distributed as a Poisson point distribution, and Λ'_{D2D} is the intensity of the co-frequency D2D UEs. The $Q(\xi, \alpha)$ function is:

$$\begin{aligned}
Q(\xi, \alpha) &= \int_{\xi^{-2/\alpha}}^{+\infty} \frac{\xi^{2/\alpha}}{1+u^{\alpha/2}} du \\
&= \sqrt{\xi} \arctan(\sqrt{\xi}) \quad \text{for } \alpha = 4.
\end{aligned} \tag{24}$$

Substituting in the expressions for $\mathcal{L}(\beta_{\text{D2D}} r_{i,j'}^\alpha)$ in Eq.23 and $I_{\text{BS}}(r_{o,j'})$ in Eq.3 of Appendix A, into Eq.22 gives the success communication probability for any single hop as:

$$\mathbb{P}_{\text{Success}} = \exp\left\{-\beta_{\text{D2D}} r_{j,j'}^\alpha P_{\text{BS}} \lambda_{\text{BS}} r_{o,j'}^{-\alpha} - \frac{P_{\text{BS}} \lambda_{\text{BS}}}{P_{\text{D2D}} \lambda_{\text{D2D}}} r_{j,j'}^\alpha \left[\frac{\pi \Lambda_{\text{BS}} \Xi(r_{o,j'}, \Psi, 4)}{2\text{erfc}^{-1}(0.5)}\right]^2 - \Lambda'_{\text{D2D}} \pi r_{i,j'}^2 Q(\xi, \alpha)\right\}. \tag{25}$$

8. References

- [1] X. Lin, J. Andrews, A. Ghosh, and R. Ratasuk, “An overview of 3GPP Device-to-Device proximity services,” *IEEE Communications Magazine*, vol. 52, no. 4, pp. 40–48, May 2014.
- [2] D. Feng, L. Lu, Y. Yi, G. Li, G. Feng, and S. Li, “Device-to-Device communications underlaying cellular networks,” *IEEE Transactions on Communications*, vol. 61, no. 8, pp. 3541–3551, Aug. 2013.
- [3] P. Phunchongharn, E. Hossain, and D. I. Kim, “Resource allocation for Device-to-Device communications underlaying lte-advanced networks,” *IEEE Wireless Communications*, vol. 20, no. 4, pp. 91–100, Aug. 2013.
- [4] M. Simsek, A. Merwaday, N. Correal, and I. Guvenc, “Device-to-Device Discovery Based on 3GPP System Level Simulations,” in *IEEE Global Communications Conference (Globecom)*, Atlanta, Jun. 2013, pp. 555 – 560.
- [5] L. Wang, H. Wu, Y. Ding, W. Chen, and H. Poor, “Hypergraph based wireless distributed storage optimization for cellular D2D underlays,” *IEEE Journal on Selected Areas of Communications (JSAC)*, 2016.

- [6] B. Bai, L. Wang, Z. Han, W. Chen, and T. Svensson, "Caching based socially-aware D2D communications in wireless content delivery networks: a hypergraph framework," *IEEE Wireless Communications*, vol. 23, no. 4, pp. 74–81, 2016.
- [7] L. Wang, H. Tang, and M. Cierny, "Device-to-device link admission policy based on social interaction information," *IEEE Transactions on Vehicular Technology*, vol. 64, no. 9, pp. 4180–4186, 2015.
- [8] A. Bhorkar, M. Naghshvar, T. Javidi, and B. Rao, "Adaptive opportunistic routing for wireless Ad Hoc networks," *IEEE/ACM Transactions on Networking*, vol. 20, no. 1, pp. 243–256, Feb. 2012.
- [9] Y. Duan, C. Li, C. Guo, Z. Liu, L. Zhu, X. Fei, and S. Ullah, "Finding the shortest path in huge data traffic networks: A hybrid speed model," in *2015 IEEE International Conference on Communications (ICC)*. IEEE, 2015, pp. 6906–6911.
- [10] Z. Chang and T. Ristaniemi, "Efficient use of multicast and unicast in collaborative OFDMA mobile cluster," in *IEEE Vehicular Technology Conference*, Dresden, Jun. 2013, pp. 1–5.
- [11] W. Guo and I. J. Wassell, "Capacity-Outage-Tradeoff for cooperative networks," *IEEE Journal on Selected Areas in Communications (JSAC)*, vol. 30, no. 9, pp. 1641–1648, Oct. 2012.
- [12] J. Sachs, I. Maric, and A. Goldsmith, "Cognitive Cellular Systems within the TV Spectrum," in *IEEE New Frontiers in Dynamic Spectrum (DYSPAN)*, Singapore, 2010, pp. 1–12.
- [13] S. P. Hyunkee Min, Jemin Lee and D. Hong, "Capacity enhancement using an interference limited area for Device-to-Device uplink underlaying cellular networks," *IEEE Transactions on Wireless Communications*, vol. 10, no. 12, pp. 3395–4000, Dec. 2011.
- [14] H. Yuan, W. Guo, and S. Wang, "Emergency route selection for D2D cellular communications during an urban terrorist attack," in *IEEE International Conference on Communications Workshops (ICC)*, Sydney, Jun. 2014, pp. 237–242.
- [15] Q. Du, H. Song, Q. Xu, P. Ren, and L. Sun, "Interference-controlled d2d routing aided by knowledge extraction at cellular infrastructure towards ubiquitous cps," *Personal and Ubiquitous Computing*, vol. 19, no. 7, pp. 1033–1043, 2015.
- [16] L. Zhu, C. Li, Y. Wang, Z. Luo, Z. Liu, B. Li, and X. Wang, "On stochastic analysis of greedy routing in vehicular networks," *IEEE Transactions on Intelligent Transportation Systems*, vol. 16, no. 6, pp. 3353–3366, 2015.
- [17] Q. Xu, P. Ren, H. Song, and Q. Du, "Security enhancement for iot communications exposed to eavesdroppers with uncertain locations," *IEEE Access*, vol. 4, pp. 2840–2853, 2016.
- [18] Y. Wu, W. Guo, H. Yuan, L. Li, S. Wang, X. Chu, and J. Zhang, "Device-to-Device (D2D) meets LTE-Unlicensed," *IEEE Communications Magazine*, vol. 54, no. 5, pp. 154–159, 2016.
- [19] M. Haenggi, *Stochastic Geometry for Wireless Networks*. England, UK: Cambridge Uni. Press, 2012.
- [20] S. Wang, W. Guo, and M. D. McDonnell, "Downlink interference estimation without feedback for heterogeneous network interference avoidance," in *International Conference on Telecommunications (ICT)*, Lisbon, May 2014, pp. 82–87.

- [21] 3GPP, “Further advancements for E-UTRA physical layer aspects (rel.9),” 3GPP TR36.814v9, Technical Report, Mar. 2010.
- [22] K. J. Zou, M. Wang, K. W. Yang, J. Zhang, W. Sheng, Q. Chen, and X. You, “Proximity discovery for Device-to-Device communications over a cellular network,” *IEEE Communications Magazine*, vol. 52, no. 6, pp. 98 – 107, 2014.
- [23] S. De, “On hop count and euclidean distance in greedy forwarding in wireless ad hoc networks,” *IEEE Communications Letters*, vol. 9, no. 11, pp. 1000–1002, Nov. 2005.
- [24] S. Andreev, A. Pyattaev, K. Johnsson, O. Galinina, and Y. Koucheryavy, “Cellular traffic offloading onto network-assisted device-to-Device connections,” *IEEE Communications Magazine*, vol. 52, no. 4, pp. 20–31, Apr. 2014.